

# Characterization and Application of Calcium-Dependent $\beta$ -Propeller Phytase from *Bacillus amyloliquefaciens* DS11

Jae-Hoon Shim<sup>†</sup> and Byung-Chul Oh<sup>\*,‡</sup>

<sup>†</sup>Department of Food Science and Nutrition, Hallym University, Hallymdaehak-gil, Chuncheon, Gwangwon-do, 200-702, Korea

<sup>‡</sup>Lee Gil Ya Cancer and Diabetes Institute, Department of Medicine, Gachon University, 7-45 Songdo-dong, Yeonsu-ku, Incheon 406-840, Korea

**ABSTRACT:** The enzyme phytase has broad biotechnological applications, especially in the reduction of phytate, antinutritional factors that chelate essential minerals, in human and animal food. We investigated the enzymatic properties of  $\beta$ -propeller phytase (BPP) from *Bacillus amyloliquefaciens* DS11. Thermal refolding analysis demonstrated that BPP can remarkably restore its enzymatic activity in the presence of 5 mM  $\text{Ca}^{2+}$  to 87% of its original activity after heating to 100 °C and subsequent cooling, indicating that the enzyme requires  $\text{Ca}^{2+}$  for appropriate refolding. Furthermore, pH-dependent kinetic studies showed that BPP required excess  $\text{Ca}^{2+}$  for its enzymatic activity as the pH decreased, suggesting that the optimal  $\text{Ca}^{2+}$ –phytate ratio for enzymatic catalysis depends on the pH value of the environment. Finally, we verified the practical application of BPP at two different pH's using soybean meal as a natural source of phytate. As compared to a commercial phytase, BPP efficiently hydrolyzed food phytate over neutral pH ranges.

**KEYWORDS:**  $\beta$ -propeller phytase,  $\text{Ca}^{2+}$ –phytate salts, thermal refolding

## ■ INTRODUCTION

Phytase (*myo*-inositol hexaphosphate phosphohydrolase) is the primary enzyme responsible for the degradation of phytates, the principal source of phosphorus in many plant tissues, especially bran and seeds.<sup>1,2</sup> This enzyme is of interest for biotechnological applications, especially for the hydrolysis of phytate in food and feedstuff, because phytate is a strong chelator of cations and binds nutritionally important divalent-cations such as  $\text{Ca}^{2+}$ ,  $\text{Co}^{2+}$ ,  $\text{Cu}^{2+}$ ,  $\text{Mg}^{2+}$ ,  $\text{Mn}^{2+}$ , and  $\text{Zn}^{2+}$  into stable metal–phytate complexes.<sup>3</sup> Monogastric animals such as humans, fish, poultry, and swine secrete insufficient quantities of enzymes into their digestive tracts to fully hydrolyze phytate salts, and instead eliminate the mineral–phytate complexes in their feces.<sup>4–9</sup> The loss of phytate salts contributes to the antinutritional impact of phytate and may result in mineral deficiencies in monogastric animals whose staple diet includes foods with high phytate contents.<sup>10–12</sup> More specifically, phytate inhibits calcium absorption in animals, leading to diseases such as rickets in dogs. Therefore, the bioavailability of minerals and phosphorus in plant foods and animal feeds would be improved if phytate were efficiently degraded.<sup>13,14</sup>

Phytases are a class of inositol-phosphate phosphatases that are responsible for the hydrolysis of phytate. Specifically, the  $\beta$ -propeller phytases (BPPs) are very useful in biotechnology and nutritional applications because they have high thermal stability, an optimal pH of approximately 7.0–8.0, and strict substrate specificity for phytate.<sup>1,2</sup> Most importantly, BPP requires  $\text{Ca}^{2+}$  ions for both enzyme activation and substrate recognition. Notably, these enzymes are also dependent on calcium ions for thermal stability. They also hydrolyze insoluble  $\text{Ca}^{2+}$ –phytate salts and completely abrogate the ability of phytate to chelate metal ions.<sup>15</sup> Although BPP has been characterized relatively well, the practical properties of BPP are not fully characterized for its application in the food and animal feed industry. In this

study, we investigated the thermal refolding and pH-dependent catalytic properties of BPP from soybean meal, a natural source of phytate, and compared its catalytic properties to those of a commercially available phytase, Natuphos.

## ■ MATERIALS AND METHODS

**Protein Preparation and the Phytase Assay.** Alkaline phytase from *Bacillus amyloliquefaciens* DS11 was prepared according to our previous reports.<sup>1,2</sup> Cells were harvested after 4–5 h and lysed by sonication in buffer containing 50 mM Tris-HCl (pH 7.6) and 5 mM  $\text{CaCl}_2$ . The BPP was purified using Ni-NTA (Qiagen, Valencia, CA) resins packed in a Poly-Prep chromatography column (Bio-Rad, Hercules, CA). Phytase activity was assayed by measuring the rate of increase in inorganic orthophosphate ( $\text{P}_i$ ) using molybdovanadate as a coloring reagent.<sup>16</sup> The experiments were conducted in 100 mM Tris-HCl (pH 7.0) under conditions in which the sodium inositol hexakisphosphate (phytate) concentration (0.01–5.0 mM) and the  $\text{Ca}^{2+}$  concentration (0–9.0 mM) varied. Sodium phytate (P-3168 from rice,  $\geq 95\%$  phosphorus basis) and calcium chloride dehydrate (C-7902, 99%) were purchased from Sigma-Aldrich Co. (St. Louis, MO). To measure activation by  $\text{Ca}^{2+}$  ions, a Chelex 100 resin (Na form; 200–400 mesh; Bio-Rad) was added to each solution and stirred for 60 min to remove contaminating  $\text{Ca}^{2+}$  ions. After filtration, the pH of the solution was checked and readjusted, if necessary, with 0.1 N HCl or 0.1 N NaOH. One unit (U) of phytase activity was defined as the amount of enzyme required to liberate 1  $\mu\text{mol}$  of phosphate per min under assay conditions.<sup>17</sup>

**Site-Directed Mutagenesis.** Mutations D56A, D56E, D56L, D308A, and D308E were performed using the megaprimer method,<sup>18</sup> where D denotes aspartic acid, and A, E, and L denote alanine, leucine, and glutamic acid. The primers used are listed in

Received: May 29, 2012

Revised: July 6, 2012

Accepted: July 9, 2012

Published: July 9, 2012

**Table 1. Oligonucleotides Used To Generate Phytase Mutants<sup>a</sup>**

name	oligonucleotide sequence
D55A	5'-GATGCA GCTGAT <u>GCGCCTGCGATT</u> TGGCT-3'
D56E	5'-GATGCAGCTGATGA <u>ACCTGCGATT</u> TGGCT-3'
D56L	5'-CCGGTGATGCAGCAGAT <u>CTTCTGCGATT</u> TGGC-3'
D308A	5'-GACGGGCTGAACAG <u>CCGGCACA</u> AGCGATA-3'
D308E	5'-GGGCCTGAAACAG <u>GGGCACA</u> AGCGATA-3'
N-term	5'-GAACATATGTCTGATCCTTATCATT-3'
C-term	5'-GAAAGCTTATTTCCGCTTCTGTCGG-3'

<sup>a</sup>The mutation sites are underlined.

Table 1. All mutations were confirmed by dideoxy chain-termination sequencing using an ABI PRISM 3700 DNA analyzer (Applied Biosystems, Foster City, CA).

**Differential Scanning Calorimetry.** The melting temperature ( $T_m$ ) of each enzyme was determined using differential scanning calorimetry (DSC, Seiko Co., Chiba, Japan).<sup>19–21</sup> All samples were scanned at a protein concentration of 50 mg/mL. The temperature scanning speed was 1 °C/min. The peak temperature at which the first derivative of each transition curve was zero was regarded as the apparent melting temperature. The curve analysis was performed using the software Disk Material Analysis System Version 3.4, which was supplied with the instrument. The reversibility of denaturation of the enzyme was probed by temperature rescanning after cooling the samples to 25 °C at a rate of 5 °C/min.

**Determination of Protein Concentration.** The protein concentration was determined by the Bradford method using bovine serum albumin as standard.<sup>22</sup> The purity of BPP was determined using 10% sodium dodecyl sulfate polyacrylamide gel electrophoresis (SDS-PAGE).

**Kinetic Analysis.** Initial velocities at fixed levels of activator and in the absence of inhibitors were fitted using the Michaelis–Menten equation. When  $\text{Ca}^{2+}$  was varied at a fixed concentration of substrate, data were analyzed using the Hill equation:

$$v = VA^h / (K_a^h + A^h) \quad (1)$$

$$v = VA^h / (K_a^h (1 + A/K_i) + A^h) \quad (2)$$

where  $V$  is the maximal velocity,  $A$  is the concentration of metal ion,  $h$  is the Hill coefficient, and  $K_a$  is the concentration of metal ion at half-maximal velocity. If necessary, a term was included in eq 2 to account for inhibition at a higher concentration of  $\text{Ca}^{2+}$  ions.

When the  $\text{Ca}^{2+}$  inhibition was determined, the concentration of metal ions was varied at saturating levels of substrate (1.8 mM), where  $K_i$  is the inhibition constant of the uncompetitive inhibitor, and  $I$  is the concentration of the competitive inhibitor. The  $\text{p}K_i$  profiles for  $\text{Ca}^{2+}$  were fitted to eq 3, because the pH profiles are constant above a single  $\text{p}K$ , but decrease with a +1 unit slope below the  $\text{p}K$ .

$$\text{p}K_i = \text{p}K_i^* - \log(1 + I/K_i) \quad (3)$$

When the  $\log V$  profile was bell-shaped with a slope of +1 at the acidic side and -1 at the basic side, the data were fitted to eq 4.

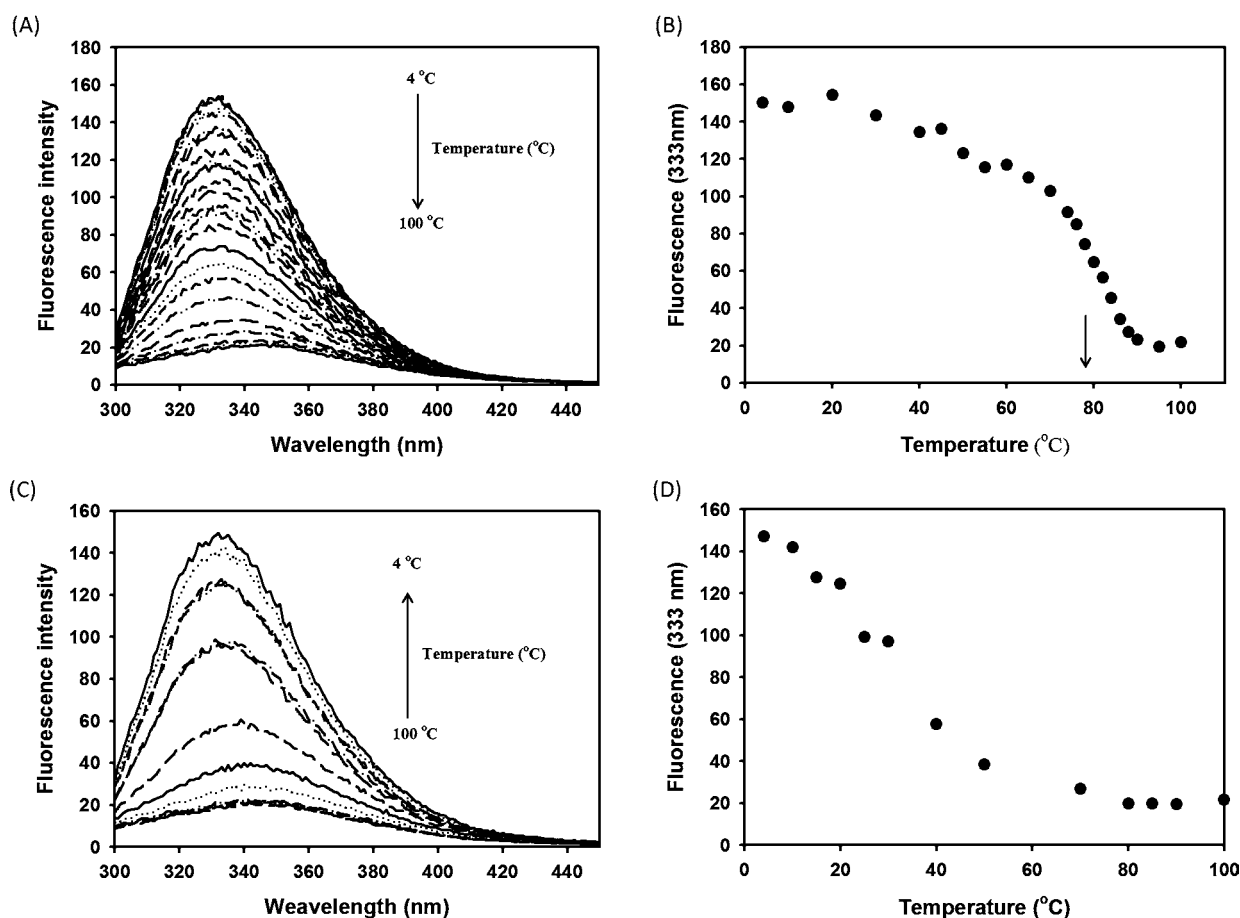


**Figure 1.** The effect of changing temperature on the fluorescence emission of BPP. Emission spectra (300–450 nm) were analyzed while raising and lowering the temperature between 4 and 100 °C with a heating or cooling rate of 1 °C/min using an excitation wavelength of 285 nm. The maximum fluorescence emission at 333 nm decreased slightly at a constant rate up to 70 °C in the presence of 5 mM  $\text{CaCl}_2$ . Above 70 °C, it started to unfold with a  $T_m$  of 78 °C (indicated with an arrow).

$$\log V = \log V^* - \log((1 + H/K_1 + K_2/H)) \quad (4)$$

When the  $\log V/K$  profile exhibited a slope of +1 at the acidic side and -1 at the basic side, the data were fitted to eq 5.

$$\log V/K = \log(V/K)^* - \log(1 + H/K_2 + K_1/H) \quad (5)$$

In eqs 3–5, the  $pK_a$ ,  $\log V^*$ , and  $\log(V/K)^*$  were the pH-independent values of the parameters, and  $K_1$  and  $K_2$  were the apparent dissociation constants for the enzyme functional group. In all cases, the best fit to the data was chosen on the basis of the standard error of the fitted parameter. Curve fitting was carried out using the programs SigmaPlot 7.0 (SPSS Inc., Chicago, IL), Origin 5.0 (OriginLab, Northampton, MA), and ENZFITTER (Biosoft, UK). The enzymatic reaction was performed with  $\text{Ca}^{2+}$  ions at various concentrations.<sup>23</sup> Kinetic parameters such as  $V_{\max}$ ,  $K_m$ , and  $K_i$  were evaluated using the nonlinear regression method based on a previously described inhibition equation.<sup>24</sup>

**pH Studies.** To avoid changing the composition of the buffer and ionic strength of the reaction mixture at various pH's, the buffer systems for pH profiles consisted of sodium acetate at pH 3.6–5.5, Bis-Tris (pH 5.5–7.0), Tris (pH 7.0–8.5), and Ches (pH 8.5–10.3). Overlaps were used in all cases, and checks were made to ensure that buffers did not interact with metal ions. The ionic strength of the mixture was 100 mM. The stability of phytase was tested under various

assay conditions by varying  $\text{Ca}^{2+}$  over a concentration range that covered both the activation and the inhibition phases, and fitting the data using eq 1 or 2. The  $K_m$  was subsequently determined by varying the substrate levels at the concentration of  $\text{Ca}^{2+}$  that gave the maximal rate at each pH.

**Enzymatic Hydrolysis of Defatted Soybean Meal.** Defatted soybean meal was purchased from Parent Seed Farms (Canada). Phytate hydrolysis was performed with 30% (w/v) defatted soybean meal in a pH stat chamber (718 Stat Titrino, Metrohm, Switzerland) to maintain the reaction constant at 50 mM sodium acetate buffer pH 5.5 or 50 mM Tris HCl pH 7.0 at 37 °C, because high amounts of released phosphate from phytate hydrolysis decrease the reaction pH. Both BPP and commercial phytase (Natuphos, BASF, Ludwigshafen, Germany) were added at concentrations of 500, 5000, and 50 000 U/kg soybean meal, respectively. The phytase units used for these studies were determined at the pH optimum of each enzyme. The enzymatic reaction was stopped at specific time points, and inorganic orthophosphate ( $\text{P}_i$ ) was measured as described previously.

**Fluorescence Measurements.** Fluorescence spectra were measured using a Shimadzu RF5301-PC equipped with a temperature controller (Yokokawa, Japan). Protein samples (100  $\mu\text{g}/\text{mL}$ ) were prepared in 20 mM Tris/HCl buffer (pH 7.0) containing 5 mM  $\text{CaCl}_2$ . The emission spectra (300–450 nm) were performed by raising the temperature from 4 to 100 °C at a rate of 1 °C/min using an excitation wavelength of 285 nm. The reversibility of denatured enzyme was probed by cooling the samples from 100 to 4 °C at a rate of 1 °C/min.

**Table 2. Kinetic Parameters for High-Affinity  $\text{Ca}^{2+}$  Binding of Wild-type and Mutant Phytases**

enzymes	$k_{\text{cat}}$ ( $\text{min}^{-1}$ )	$K_m$ (mM)	$k_{\text{cat}}/K_m$ ( $\text{min}^{-1}/\text{mM}^{-1}$ )	relative activity (%)
wild-type	992.8 $\pm$ 5.20	0.138 $\pm$ 0.022	7194.49	100.00
D56A	4.0 $\pm$ 0.02	0.248 $\pm$ 0.032	16.12	0.40
D56E	200.4 $\pm$ 0.84	0.189 $\pm$ 0.043	26.53	20.21
D56L	6.0 $\pm$ 0.08	0.218 $\pm$ 0.084	1060.32	0.59
D308A	500.0 $\pm$ 2.84	0.167 $\pm$ 0.052	2994.01	50.38
D308E	933.2 $\pm$ 1.14	0.156 $\pm$ 0.032	5982.05	94.04

**Table 3.  $T_m$  Values and Optimal Temperature of BBP and BBP Mutant Enzymes**

enzymes	$T_m$ (°C)		optimum temperature (°C)
	EDTA	5 mM $\text{CaCl}_2$	
wild-type	48.8	80.1	80
D56A	ND <sup>a</sup>	48.8	ND
D56E	ND	55.5	60
D56L	ND	49.6	50
D308A	ND	48.6	50
D308E	ND	54.8	55

<sup>a</sup>ND: not detected.

**Table 4. pH Dependence of the Kinetic Parameters of Phytase**

pH	$k_{\text{cat}}$ ( $\mu\text{mol}/\text{min}^{-1}$ )	$K_m$ ( $\mu\text{M}$ )	$K_a$ (mM)	$\text{Ca}^{2+}_{\text{opt}}/\text{phytate}$ (mM)	$K_i \text{Ca}^{2+}$ (mM)
4	13.1 $\pm$ 1.43	0.159 $\pm$ 0.02	13.68 $\pm$ 0.89	35.0	738.0 $\pm$ 9.86
4.5	16.6 $\pm$ 0.34	0.154 $\pm$ 0.01	3.66 $\pm$ 0.40	15.0	197.2 $\pm$ 2.40
5	21.0 $\pm$ 0.44	0.151 $\pm$ 0.03	0.81 $\pm$ 0.01	3.0	43.6 $\pm$ 3.63
5.5	22.6 $\pm$ 0.21	0.148 $\pm$ 0.03	0.44 $\pm$ 0.03	2.0	23.7 $\pm$ 3.26
6	24.0 $\pm$ 0.22	0.146 $\pm$ 0.01	0.33 $\pm$ 0.05	2.0	17.6 $\pm$ 1.26
6.5	24.3 $\pm$ 0.36	0.137 $\pm$ 0.01	0.30 $\pm$ 0.01	2.0	11.1 $\pm$ 1.13
7	25.0 $\pm$ 0.28	0.134 $\pm$ 0.02	0.14 $\pm$ 0.01	1.0	7.4 $\pm$ 0.68
7.5	25.0 $\pm$ 0.26	0.136 $\pm$ 0.01	0.17 $\pm$ 0.03	1.0	6.9 $\pm$ 0.55
8	22.5 $\pm$ 0.17	0.143 $\pm$ 0.02	0.19 $\pm$ 0.01	1.0	5.2 $\pm$ 0.45
8.5	19.4 $\pm$ 0.25	0.157 $\pm$ 0.02	0.25 $\pm$ 0.04	1.0	4.6 $\pm$ 0.65
9	16.1 $\pm$ 0.22	0.163 $\pm$ 0.03	0.50 $\pm$ 0.03	2.0	4.5 $\pm$ 0.52
9.5	12.1 $\pm$ 1.24	0.174 $\pm$ 0.02	0.83 $\pm$ 0.05	2.0	4.5 $\pm$ 0.72

## RESULTS AND DISCUSSION

**Thermal Unfolding and Refolding of BPP.** The thermal stability of enzymes is important for the food industry and for animal feedstuff processing.<sup>17,25–27</sup> To investigate the structural properties and conformational changes of BPP by heating and subsequent cooling, thermal denaturation of BPP by heating was analyzed by tryptophan fluorescence. The results of a BPP typical tryptophan fluorescence emission experiment in the presence of 5 mM  $\text{CaCl}_2$  are shown in Figure 1. The fluorescence emission intensity slightly decreased by heating to 70 °C, while a drastic transition in fluorescence emission intensity was observed in the temperature range from 70 to 90 °C with a  $T_m$  of 79 °C. The dramatic transition of fluorescence emission indicated that BPP started to unfold at 70 °C and rapidly lost its catalytic activity. In contrast, thermal refolding experiments were performed by decreasing the temperature from 100 to 4 °C at a rate of 1 °C/min. As shown in Figure 1C, the fluorescence emission intensity of BPP increased as the temperature decreased. Surprisingly, about 87% of the original activity of BPP was restored. The fluorescence emission intensity rapidly increased by cooling the temperature below 50 °C and BPP quickly recovered its catalytic activity (Figure 1D).

Furthermore, the thermal refolding properties of BPP are highly attractive for food processing because cereal or animal feed is commonly sterilized to control microbial growth.<sup>28</sup>

To determine the roles of critical amino acids in  $\text{Ca}^{2+}$  binding, we substituted the aspartic acid residues Asp56 and Asp308 with alanine (A), leucine (L), or glutamic acid (E) by site-specific mutagenesis based on structural information.<sup>19</sup> These mutants were purified to homogeneity, and their kinetic parameters were determined. Table 2 summarizes the kinetic parameters obtained from the wild-type and mutant phytase. The mutations resulted in decreased catalytic activity: mutation of D56A and D56L resulted in a total reduction in activity, indicating that residue asp56 is critical, while mutation of D308A and D308E retained 50% and 94% of the wild-type activity, respectively. In addition, the enzyme activity was measured at various temperatures ranging from 20 to 100 °C in 100 mM Tris/HCl (pH 7.0) in an oil bath. Typically, the mutant enzymes exhibited reduced optimal temperatures where mutations were introduced at the high-affinity  $\text{Ca}^{2+}$  binding site (Table 3). The optimal temperature of D56A, D56L, and D308A mutant enzymes decreased by 30 °C as compared to the wild-type enzyme, while the D56E and D308E mutant enzymes had an optimal temperature of 60 and 55 °C, respectively. The  $T_m$  value of each mutant in the presence of 5 mM  $\text{CaCl}_2$  was also determined by DSC. As compared to wild-type BPP, D56E and D308A had about a 25 °C decrease in  $T_m$  values, whereas the  $T_m$  values of D56A, D56L, and D308A were decreased by 30.5–31.5 °C (Table 3). The thermostability of each mutant enzyme, as measured by DSC, agreed with that obtained by the optimal assay temperature analysis, suggesting that physical unfolding was the cause of both the reduced catalytic activity and the decreased optimal temperature. These results, in conjunction with the thermal stability data, clearly indicate that binding of  $\text{Ca}^{2+}$  increases the thermal stability of BPP as well as the enzymatic activity of the propeller structure.

#### pH Dependence of the Kinetic Parameters of Phytases.

In addition to the enzymatic activity and thermal stability of BPP, our previous study using isothermal titration calorimetry (ITC) indicated that phytate binds  $\text{Ca}^{2+}$  ion in a pH range of 3.0–9.0 and that maximal high-affinity  $\text{Ca}^{2+}$  binding is observed at pH 4.0.<sup>15</sup> Furthermore, all phytates exist as monocalcium–phytate or tricalcium–phytate in the presence of  $\text{Ca}^{2+}$  ions.<sup>15</sup> Thus, phytate forms  $\text{Ca}^{2+}$ –phytate complexes easily in food or animal feedstuffs. To investigate the effects of  $\text{Ca}^{2+}$  concentration on BPP activity over the entire pH range, we performed pH-dependent kinetic studies of BPP with varying  $\text{Ca}^{2+}$  levels and fixed amounts of phytate. We determined the concentration of  $\text{Ca}^{2+}$  optimal for phytate activity at different pH's. The pH dependence of  $\log V$ ,  $\log V/K$ ,  $\text{Ca}^{2+}$  inhibition constant, and optimum  $\text{Ca}^{2+}$ /phytate ratio for phytase activity are summarized in Table 4. The data for  $\log V$  fit well to a bell-shaped curve with slopes of +1 and –1 on the acidic and basic sides, respectively, using eq 4. This indicates that  $\log V$  depends on two ionizing groups with  $\text{pK}_a$  values of  $\sim 3.94$  and  $\sim 9.47$  (Figure 2A). Data for the pH dependence of  $\log V/K$  fit best using eq 5 to a bell-shaped curve with slopes of +2 and –1 on the acidic and basic sides, respectively, indicating dependence on three ionizing groups with  $\text{pK}_a$  values of  $\sim 3.84$ ,  $\sim 4.74$ , and  $\sim 9.54$  (Figure 2B). The pH profile of  $\text{pK}_i$  for  $\text{Ca}^{2+}$  was a half-bell with a limiting slope of +1 on the acidic side (Figure 2C). The data fit to eq 3 to yield a  $\text{pK}_a$  value of  $\sim 4.93$ . The pH profiles of  $\text{pK}_i$  for  $\text{Ca}^{2+}$ , a competitive inhibitor, showed that a single residue with a  $\text{pK}_a$  value of 4.93 might be ionized in the

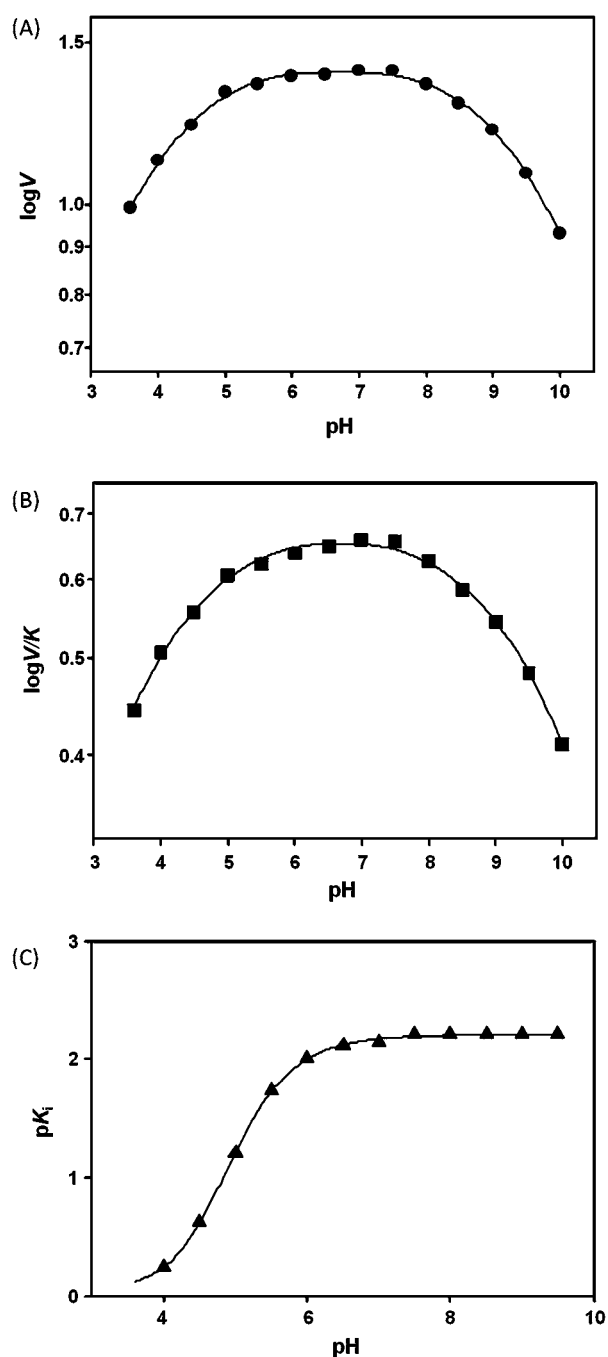


**Figure 2.** The pH dependence of kinetic parameters and  $\text{Ca}^{2+}$  inhibition constants. Initial velocity was measured at 37 °C as described in the Materials and Methods.  $V$  was determined in the presence of 1.8 mM phytate by varying  $\text{Ca}^{2+}$  over the concentration range that covered both activation and inhibition phases, and fitting the data using eq 1 or 2.  $K_m$  was subsequently determined by varying the substrate at the concentration of  $\text{Ca}^{2+}$  giving the maximal rate obtained with 1.8 mM sodium phytate at each pH. The  $\text{pK}_i$  equals  $\log 1/K_i$ ;  $K_i$  is denoted as moles per liter.

presence of excess  $\text{Ca}^{2+}$  or  $\text{Ca}^{2+}$ –phytate. The concentration of  $\text{Ca}^{2+}$  required to reach the half-maximal activation increased from 0.138 mM at pH 7.0 to 13.68 mM at pH 3.6, probably due to protonation of the phosphate groups of phytate or  $\text{Ca}^{2+}$  binding residues of the enzyme. Hill constants remained unchanged over the entire pH range. From these pH-dependent kinetics, the pH profiles of the catalytic activity of BPP showed

that this enzyme is highly active at a pH range of 5.0–8.0 (Figure 2A). Furthermore, excess  $\text{Ca}^{2+}$  was required at pH values less than 5.0, indicating that the optimal  $\text{Ca}^{2+}$ –phytate ratio for enzymatic activity increased as pH decreased (Figure 3). These results indicate that free phytate is not a

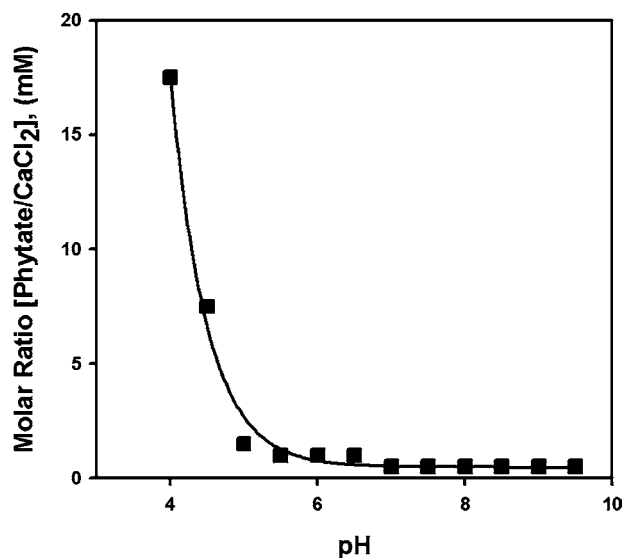


**Figure 3.** The pH dependence of optimal  $\text{Ca}^{2+}$ –phytate ratio. Each point was determined by varying the  $\text{Ca}^{2+}$  concentration in the vicinity of its  $K_m$  at 1.8 mM sodium phytate concentration, and fitting the initial velocities using eq 3.

substrate for BPP, and that the true substrate is  $\text{Ca}^{2+}$ –phytate.<sup>2</sup> Taken together, these results suggest that BPP is capable of hydrolyzing  $\text{Ca}^{2+}$ –phytate in phytate-rich foods containing  $\text{Ca}^{2+}$ , even at acidic pH's.

#### Time Course Analysis for Natural Phytate Utilization.

The results thus far presented demonstrate that BPP requires  $\text{Ca}^{2+}$  ions for its thermal stability and catalytic activity over broad pH ranges. To address whether BPP is capable of hydrolyzing phytate-rich foods where most phytate is present as a  $\text{Ca}^{2+}$ –phytate complex, we performed enzymatic hydrolysis at two different pH's using soybean meal, and compared the catalytic activities of BPP and Natuphos. As shown in Figure 4A, both BPP and Natuphos liberated similar amounts of phosphate from soybean meal in an enzyme dose-dependent manner. However, although BPP showed highly dose-dependent enzyme activity, under identical conditions Natuphos did not liberate additional phosphate even with more enzyme present. These results indicate that the catalytic activity of Natuphos decreased due to the presence of either excess hydrolytic products, inorganic phosphate, or excess minerals at neutral pH where most phytate in foods exists as  $\text{Ca}^{2+}$ –phytate.<sup>17</sup> This agrees with previous results that Natuphos rarely hydrolyzes food phytate at neutral pH.<sup>1,2,29</sup> However, in the gastrointestinal tract, Natuphos hydrolyzes food phytate more efficiently than in vitro food processing. In contrast, we did not find that BPP was inhibited by inorganic phosphate. At neutral conditions of pH 7.0, BPP hydrolyzed soybean meal more efficiently than Natuphos, indicating that BPP hydrolyzes  $\text{Ca}^{2+}$ –phytate salts in soybean meal (Figure 4B).<sup>30–32</sup> The results suggest that BPP is a strong candidate for phytate reduction in the food and animal feed industry such as soybean milk processing and starch hydrolysis.<sup>33,34</sup> In conclusion, BPP showed high thermal

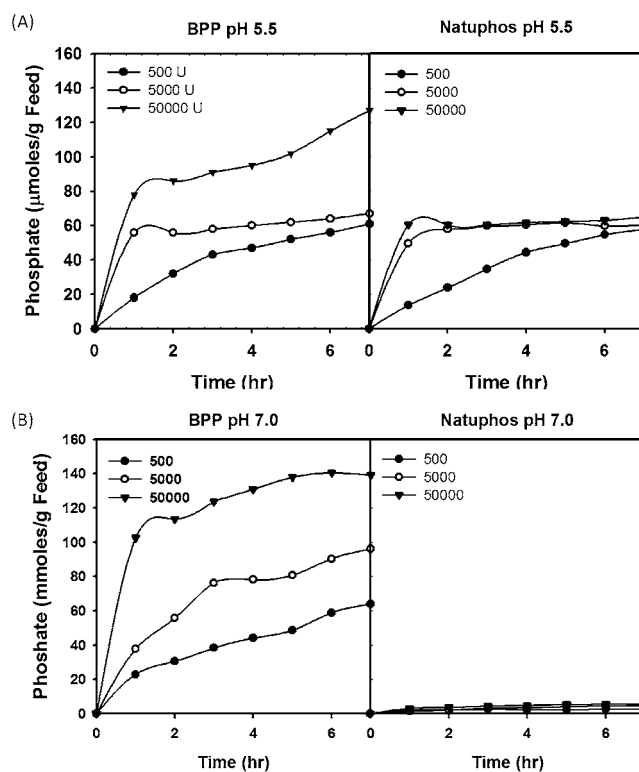


**Figure 4.** Comparative enzyme activity of BPP and Natuphos at pH 5.5 (A) and pH 7.0 (B). Time course for inorganic phosphate formation using soybean meal at concentrations of 500 U/kg (●), 5000 U/kg (○), and 50 000 U/kg (▼). The reaction was stopped at the indicated time points. Data points represent the mean of eight determinations.

stability and catalytic activity over neutral pH ranges. Most importantly, BPP is suitable for hydrolyzing food phytate and eventually increases the  $\text{Ca}^{2+}$  availability of food.

## AUTHOR INFORMATION

### Corresponding Author

\*Tel.: 82-32-899-6074. Fax: 82-32-899-6075. E-mail: bcoh@gachon.ac.kr.

### Funding

This study was supported in part by the 21C Frontier Microbial Genomics and Applications Center Program (11-2008-18-001-00 to B.-C.O.) and the Basic Science Research Program (NRF-2010-0024500 to B.-C.O. and NRF-2011-0009695 to J.-H.S.) of the National Research Foundation funded by the Korean Government.

### Notes

The authors declare no competing financial interest.

## REFERENCES

- Oh, B. C.; Chang, B. S.; Park, K. H.; Ha, N. C.; Kim, H. K.; Oh, B. H.; Oh, T. K. Calcium-dependent catalytic activity of a novel phytase from *Bacillus amyloliquefaciens* DS11. *Biochemistry* **2001**, *40*, 9669–9676.
- Oh, B. C.; Kim, M. H.; Yun, B. S.; Choi, W. C.; Park, S. C.; Bae, S. C.; Oh, T. K.  $\text{Ca}^{2+}$ -inositol phosphate chelation mediates the substrate specificity of beta-propeller phytase. *Biochemistry* **2006**, *45*, 9531–9539.
- Raboy, V. Seeds for a better future: “low phytate” grains help to overcome malnutrition and reduce pollution. *Trends Plant Sci.* **2001**, *6*, 458–462.

- (4) Erdman, J. W., Jr.; Poneros-Schneier, A. Phytic acid interactions with divalent cations in foods and in the gastrointestinal tract. *Adv. Exp. Med. Biol.* **1989**, *249*, 161–171.
- (5) Hallberg, L. Search for nutritional confounding factors in the relationship between iron deficiency and brain function. *Am. J. Clin. Nutr.* **1989**, *50*, 598–604.
- (6) Heaney, R. P.; Weaver, C. M.; Fitzsimmons, M. L. Soybean phytate content: effect on calcium absorption. *Am. J. Clin. Nutr.* **1991**, *53*, 745–747.
- (7) Lonnerdal, B.; Bell, J. G.; Hendrickx, A. G.; Burns, R. A.; Keen, C. L. Effect of phytate removal on zinc absorption from soy formula. *Am. J. Clin. Nutr.* **1988**, *48*, 1301–1306.
- (8) Reddy, N. R.; Sathe, S. H. *Food Phytates*; CRC Press: Boca Raton, FL, 2002; pp 25–51.
- (9) Sandstead, H. H. Fiber, phytates, and mineral nutrition. *Nutr. Rev.* **1992**, *50*, 30–31.
- (10) McCance, R. A.; Widdowson, E. M. Mineral metabolism on dephytinized bread. *J. Physiol.* **1942**, *101*, 304–13.
- (11) McCance, R. A.; Widdowson, E. M. Mineral metabolism of healthy adults on white and brown bread dietaries. *J. Physiol.* **1942**, *101*, 44–85.
- (12) Mellanby, E. The rickets-producing and anti-calcifying action of phytate. *J. Physiol.* **1949**, *109*, 488–533.
- (13) Brune, M.; Rossander-Hulten, L.; Hallberg, L.; Gleerup, A.; Sandberg, A. S. Iron absorption from bread in humans: inhibiting effects of cereal fiber, phytate and inositol phosphates with different numbers of phosphate groups. *J. Nutr.* **1992**, *122*, 442–449.
- (14) Navert, B.; Sandstrom, B.; Cederblad, A. Reduction of the phytate content of bran by leavening in bread and its effect on zinc absorption in man. *Br. J. Nutr.* **1985**, *53*, 47–53.
- (15) Kim, O. H.; Kim, Y. O.; Shim, J. H.; Jung, Y. S.; Jung, W. J.; Choi, W. C.; Lee, H.; Lee, S. J.; Kim, K. K.; Auh, J. H.; Kim, H.; Kim, J. W.; Oh, T. K.; Oh, B. C. beta-propeller phytase hydrolyzes insoluble Ca(2+)-phytate salts and completely abrogates the ability of phytate to chelate metal ions. *Biochemistry* **2010**, *49*, 10216–10227.
- (16) Engelen, A. J.; van der Heeft, F. C.; Randsdorp, P. H.; Somers, W. A.; Schaefer, J.; van der Vat, B. J. Determination of phytase activity in feed by a colorimetric enzymatic method: collaborative interlaboratory study. *J. AOAC Int.* **2001**, *84*, 629–633.
- (17) Park, S. C.; Oh, B. C.; Rhee, M. H.; Jeong, K. S.; Lee, K. W.; Song, J. C.; Oh, T. K. The enzyme activity of a novel phytase from *Bacillus amyloliquefaciens* DS11 and its potential use as a feed pellet. *J. Gen. Appl. Microbiol.* **2003**, *49*, 129–133.
- (18) Sarkar, G.; Sommer, S. S. The “megaprimer” method of site-directed mutagenesis. *BioTechniques* **1990**, *8*, 404–7.
- (19) Ha, N. C.; Oh, B. C.; Shin, S.; Kim, H. J.; Oh, T. K.; Kim, Y. O.; Choi, K. Y.; Oh, B. H. Crystal structures of a novel, thermostable phytase in partially and fully calcium-loaded states. *Nat. Struct. Biol.* **2000**, *7*, 147–153.
- (20) Shim, J. H.; Kim, Y. W.; Kim, T. J.; Chae, H. Y.; Park, J. H.; Cha, H.; Kim, J. W.; Kim, Y. R.; Schaefer, T.; Spindler, T.; Moon, T. W.; Park, K. H. Improvement of cyclodextrin glucanotransferase as an antistaling enzyme by error-prone PCR. *Protein Eng., Des. Sel.* **2004**, *17*, 205–211.
- (21) Shim, J. H.; Seo, N. S.; Roh, S. A.; Kim, J. W.; Cha, H.; Park, K. H. Improved bread-baking process using *Saccharomyces cerevisiae* displayed with engineered cyclodextrin glucanotransferase. *J. Agric. Food Chem.* **2007**, *55*, 4735–4740.
- (22) Bradford, M. M. A rapid and sensitive method for the quantitation of microgram quantities of protein utilizing the principle of protein-dye binding. *Anal. Biochem.* **1976**, *72*, 248–254.
- (23) Segel, I. H. *Simple Inhibition Systems in Enzyme Kinetics: Behavior and Analysis of Rapid Equilibrium and Steady-State Enzyme System*; John Wiley & Sons, Inc.: New York, 1975; pp 100–202.
- (24) Duggleby, R. G.; Leonard, D. R. *DNRPEASY, a data analysis computer program*, 1992.
- (25) Park, Y. J.; Park, J.; Park, K. H.; Oh, B. C.; Auh, J. H. Supplementation of alkaline phytase (Ds11) in whole-wheat bread reduces phytate content and improves mineral solubility. *J. Food Sci.* **2011**, *76*, C791–794.
- (26) Brinch-Pedersen, H.; Hatzack, F.; Stoger, E.; Arcalis, E.; Pontopidan, K.; Holm, P. B. Heat-stable phytases in transgenic wheat (*Triticum aestivum* L.): deposition pattern, thermostability, and phytate hydrolysis. *J. Agric. Food Chem.* **2006**, *54*, 4624–4632.
- (27) Wawire, M.; Oey, I.; Mathooko, F.; Njoroge, C.; Shitanda, D.; Hendrickx, M. Thermal stability of ascorbic acid and ascorbic acid oxidase in african cowpea leaves (*Vigna unguiculata*) of different maturities. *J. Agric. Food Chem.* **2011**, *59*, 1774–1783.
- (28) Mullaney, E. J.; Daly, C. B.; Ullah, A. H. Advances in phytase research. *Adv. Appl. Microbiol.* **2000**, *47*, 157–199.
- (29) Common, F. H. Biological availability of phosphorus for pigs. *Nature* **1989**, *143*, 370–380.
- (30) Liu, J.; Boollinger, D. W.; Ledoux, D. R.; Veum, T. L. Lowering the dietary calcium to total phosphorus ratio increases phosphorus utilization in low-phosphorus corn-soybean meal diets supplemented with microbial phytase for growing-finishing pigs. *J. Anim. Sci.* **1998**, *76*, 808–813.
- (31) Maenz, D. D.; Classen, H. L. Phytase activity in the small intestinal brush border membrane of the chicken. *Poult. Sci.* **1998**, *77*, 557–63.
- (32) Maenz, D. D.; Engele-Schaan, C. M.; Newkirk, R. W.; Classen, H. L. The effect of minerals and mineral chelators on the formation of phytase-resistant and phytase-susceptible forms of phytic acid in solution and in a slurry of canola meal. *Anim. Feed Sci. Technol.* **1999**, *81*, 177–192.
- (33) Lim, M. H.; Lee, O. H.; Chin, J. E.; Ko, H. M.; Kim, I. C.; Lee, H. B.; Im, S. Y.; Bai, S. Simultaneous degradation of phytic acid and starch by an industrial strain of *Saccharomyces cerevisiae* producing phytase and alpha-amylase. *Biotechnol. Lett.* **2008**, *30*, 2125–2130.
- (34) Tang, A. L.; Wilcox, G.; Walker, K. Z.; Shah, N. P.; Ashton, J. F.; Stojanovska, L. Phytase activity from *Lactobacillus* spp. in calcium-fortified soymilk. *J. Food Sci.* **2010**, *75*, M373–376.